Biosensors and Bioelectronics 26 (2010) 255–261

Contents lists available at ScienceDirect

Biosensors and Bioelectronics

journal homepage: www.elsevier.com/locate/bios

# A hard–soft microfluidic-based biosensor flow cell for SPR imaging application

Changchun Liu*, Dafu Cui, Hui Li

*State Key Laboratory of Transducer Technology, Institute of Electronics, Chinese Academy of Sciences, Beijing 100190, PR China*

ARTICLE INFO

*Article history:*
Received 31 March 2010
Received in revised form 19 June 2010
Accepted 23 June 2010
Available online 1 July 2010

*Keywords:*
Plastic–PDMS bonding
Microfluidic-based biosensor flow cell
SPR imaging
Immunoassay

ABSTRACT

An ideal microfluidic-based biosensor flow cell should have not only a "soft" interface for high strength sealing with biosensing chips, but also "hard" macro-to-micro interface for tubing connection. Since these properties are exclusive of each other, no one material can provide the advantages of both. In this paper, we explore the application of a $SiO_2$ thin film, deposited by plasma-enhanced chemical vapor deposition (PECVD) technology, as an intermediate layer for irreversibly adhering polydimethylsiloxane (PDMS) to plastic substrate, and develop a hard–soft, compact, robust microfluidic-based biosensor flow cell for the multi-array immunoassay application of surface plasmon resonance (SPR) imaging. This hard–soft biosensor flow cell consists of one rigid, computer numerically controlled (CNC)-machined poly(methyl methacrylate) (PMMA) base coated with a 200 nm thick $SiO_2$ thin film, and one soft PDMS microfluidic layer. This novel microfluidic-based biosensor flow cell does not only keep the original advantage of conventional PDMS-based biosensor flow cell such as the intrinsically soft interface, easy-to-fabrication, and low cost, but also has a rigid, robust, easy-to-use interface to tubing connection and can be operated up to 185 kPa in aqueous environments without failure. Its application was successfully demonstrated with two types of experiments by coupling with SPR imaging biosensor: the real-time monitoring of the immunoglobulin G (IgG) interaction, as well as the detection of sulfamethoxazole (SMOZ) and sulfamethazine (SMZ) with the sensitivity of 3.5 and 0.6 ng/mL, respectively. This novel hard–soft microfluidic device is also useful for a variety of other biosensor flow cells.



## 1. Introduction

Over the last two decades, microfluidic technology has gained significance as an interdisciplinary technology with applications in many important fields such as clinical diagnostics (Yager et al., 2006; Liu et al., 2009; Gervais and Delamarche, 2009), chemical analysis (Liu et al., 2006), food safety testing (Crevillén et al., 2007), environmental monitoring (Li and Lin, 2009) pharmaceutical drug discovery (Pihl et al., 2006), etc. Microfluidic chips offer the researcher many advantages, including high sample throughput, integrated sample processing, minimized sample and reagent volume, and increased ease of fluid manipulation. In recent years, there are strong interests on the combination of microfluidic technology with a variety of biosensors, which offers some significant advantages (Luo et al., 2008; Lee et al., 2007; Mitsakakis et al., 2009; Yoshinobu et al., 2005): (i) Microfluidic technology is well suited for automation, which allows manipulations to be sequenced and controlled for the efficiency and precision of the biosensor analysis. (ii) The use of microfluidic technology allows the biosensor-based detection to be carried out with less sample consumption. (iii) The microfluidic device provides flow channels with micro/nanolitre volumes. This feature accelerates the biochemical reactions on the biosensors due to the reduction of diffusion distances.

Poly(dimethylsiloxane) (PDMS) is becoming more popular among the microfluidic chips community because of its biocompatibility, flexibility, low cost, easy-to-fabrication and rapid sealing properties. At present, a variety of microfluidic-based biosensor flow cells are made of PDMS, including surface plasmon resonance (SPR) biosensor (Nakajima et al., 2006; Kawazumi et al., 2005; Wheeler et al., 2004), light-addressable potentiometric sensor (LAPS) (Yoshinobu et al., 2005), quartz crystal microbalance (QCM) sensor (Michalzik et al., 2005), surface acoustic wave (SAW) sensor (Mitsakakis et al., 2009), electrochemical biosensor (Varshney et al., 2007; Kjeang et al., 2007), etc. However, these PDMS-based flow cells have some significant drawbacks which hinder their use outside of the laboratory by relatively untrained users. For example, PDMS-based biosensor flow cells have generally a soft characteristic and are easy to deform, so special care should be taken in the experiment. Moreover, they cannot withstand a high pressure, which occurs when high-flow rate is applied in the biosensing experiment. Especially, their soft macro-to-micro interface for tubing connection is a challenge for untrained researcher. Usually, an ideal microfluidic-based biosensor flow cell should have not only one "soft" interface for high strength sealing with biosensing chips, but also "hard" macro-to-micro interface for tubing connection.

* Corresponding author.
*E-mail address:* liucc263@yahoo.com.cn (C. Liu).

0956-5663/$ – see front matter © 2010 Elsevier B.V. All rights reserved.
doi:10.1016/j.bios.2010.06.041

Since these properties are exclusive of each other, no one material can provide the advantages of both.

Thermoplastics have an excellent rigid characteristic and can be manufactured using mass fabrication technologies such as injection molding, computer numerically controlled (CNC) machining and hot embossing with well-established bonding processes (Liu et al., 2009, 2006; Tsao and DeVoe, 2009). Plastics are also more dimensionally stable, rigid, and chemically resistant. Its rigidity enables a variety of reliable external interface options, such as manifold integration, direct barbed tubing connections, and gasket connectors. However, plastic substrates do not generally form irreversible adhesion with PDMS even if their surface is treated in oxygen plasma due to the difference of their chemical compositions (Chow et al., 2006). There are few existing methods proposed to improve the adhering strength of PDMS to plastics. For example, Lee and Ram (2009) developed an organofunctional silanes coating method for high strength plastic–PDMS bonding. Vlachopoulou et al. (2009) introduced the Si-containing groups on poly(methyl methacrylate) (PMMA) surface through 3-aminopropyltriethoxysilane (APTES)-functionalization, and realized an irreversible bonding of PMMA–PDMS. Tang and Lee (2010) presented also a high strength plastic–PDMS bonding technology within 1 h at room temperature by the formation of a chemically robust amine–epoxy bond at the bonding interfaces. Kersey et al. (2009) evaluated the performance of an adhesion promoter (GE SS4120) coating for irreversibly bonding PDMS to plastic substrate surfaces. However, the surface chemistry modification techniques are generally a wet chemical process and intrinsically dependent on the surface chemistry composite of substrate material. The adhesion promoter coating method is a simple and universal method, but not suited for the microfluidic devices with a three-dimensional (3-D) structure. Moreover, these methods mainly focus on the direct bonding of solidified PDMS layer to plastic substrate, and are not very compatible with micro-electro-mechanical systems (MEMS) fabrication process for the mass production of BioMEMS devices. It was well known that uncured PDMS prepolymer could form irreversible bonding with glass when it was cured upon glass plate (Wu et al., 2005; Samel et al., 2007; Liu et al., 2007).

In this paper, we use a $SiO_2$ thin film, formed by PECVD dry deposition process, as an adhesion intermediate layer for PDMS irreversible adhesion to plastic substrates. A hard–soft, compact, robust, easy-to-use, PMMA–PDMS hybrid microfluidic-based biosensor flow cell for SPR imaging application was designed and fabricated. This novel, hybrid biosensor flow cell shows some distinct advantages over the previous PDMS-based biosensor flow cells including high sealing strength, easy-to-use interface, etc. Its performance is successfully demonstrated by real-time monitoring of the IgGs interaction and the detection of sulfamethoxazole and sulfamethazine by coupling with SPR imaging biosensor.

## 2. Experimental

### 2.1. Materials and reagents

PMMA and polycarbonate (PC) plate were obtained from Jiangsu Right Plastics Co. Ltd. (Changzhou, China). Cyclic olefin copolymer (COC) plate was purchased from Zeon Chemicals (Louisville, KY, USA). Human IgG, rabbit IgG, sheep anti-human IgG and sheep anti-rabbit IgG were obtained from Dingguo Biological Technology Co. (Beijing, China). Sulfamethazine, sulfamethazine–BSA conjugate and its monoclonal antibodies were the gifts from China Agricultural University. Sulfamethoxazole, sulfamethoxazole–BSA conjugate and its monoclonal antibodies were the gifts from China Institute of Atomic Energy. N-hydroxysuccinimide (NHS) and 1-ethyl-3-(3-dimethylaminopropyl)carbodiimide hydrochloride (EDC) were purchased from Acros Organics company (USA). Ethanolamine was purchased from Sigma–Aldrich (USA). Acetonitrile, sodium hydroxide and ethanol were obtained from Beijing Chemical Reagent Co. (Beijing, China). Sylgard 184 PDMS elastomer base and the curing reagent were acquired from Dow Corning Corporation (Midland, MI, USA). The HBS-EP buffer (10 mM Hepes, pH 7.4, 150 mM NaCl, 0.005% (v/v) Surfactant P20, 3 mM EDTA) was prepared in laboratory.

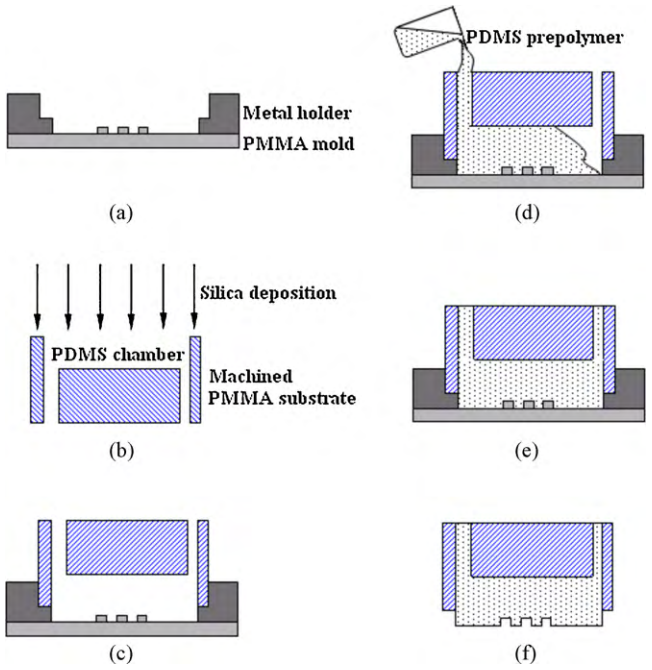


**Fig. 1.** A schematic illustration of fabrication process of hard–soft microfluidic-based biosensor flow cell: (a) metal holder was mounted on the surface of PMMA master mold; (b) the PDMS chamber in PMMA base was deposited with a 200 nm thick $SiO_2$ film by PECVD technology; (c) the PMMA base was mounted on the metal holder; (d) PDMS prepolymer was poured into PMMA base from its cast hole; (e) the cast PDMS was cured at 35 °C overnight; (f) the hard–soft microfluidic-based biosensor flow cell was released from the mold.

### 2.2. Deposition of $SiO_2$ thin film

Before depositing $SiO_2$ thin film by plasma-enhanced chemical vapor deposition (PECVD), the plastic substrate was rinsed with deionized water, cleaned by the ultrasonic cleaning device, and dried in a stream of dry nitrogen. Then, the plastic substrate was cleaned in ethanol for sonicating for 20 min, and dried in a stream of dry nitrogen. The $SiO_2$ deposition was performed at room temperature on the PECVD-801 (Beijing Chuangweina Technologies Co., Ltd.). The PECVD process used silane $SiH_4$ and dinitrogenoxide $N_2O$ for the plasma, with the following parameters: $SiH_4$ gas flow rate 30 sccm, $N_2O$ gas flow rate 36 sccm, pressure 100 mTorr and RF power 200 W for 6 min to deposit one approximately 200 nm thick $SiO_2$ layer on plastic substrates (Wuu et al., 2004). A surface profiler (Alpha-Step 500, TENCOR, USA) was used for measuring the thickness of $SiO_2$ thin film. Fourier transformation infrared (FTIR) spectra were obtained using a Bruker IFS 66V/S FTIR spectrometer.

### 2.3. Fabrication of hard–soft microfluidic-based biosensor flow cell

Fig. 1 illustrates schematically the detailed fabrication process of hard–soft microfluidic-based biosensor flow cell. One PMMA master mold cut directly by $CO_2$ laser machine was used for PDMS casting. Briefly, features of the flow cell was first designed and cre-

ated directly in a CAD program. Then, one 0.5 mm thick PMMA sheet was cut by $CO_2$ laser machine, and the laser-cut PMMA master mold was cleaned with deionized water and ethanol by the ultrasonic cleaning device, and dried in a stream of dry nitrogen. Next, laser-cut PMMA master mold was glued on the thick flat PMMA sheet by adding one drop of acetonitrile solvent. After dry for 10 min at room temperature, the PMMA master mold was ready for PDMS casting. The PMMA master mold has a wraparound feature with a 500 μm thickness and 1.0 mm width. To hold the PMMA base for PDMS casting, one CNC-machined metal holder was mounted on the surface of PMMA master mold (Fig. 1a).

The body of the PMMA base with a 25 mm length × 21 mm width × 10 mm thickness is machined by CNC milling machine. The surface of PDMS chamber in PMMA base was first deposited with a 200 nm thick $SiO_2$ film by PECVD (Fig. 1b). Then, PMMA base was immediately mounted on the metal holder for PDMS casting (Fig. 1c). A 10:1 mixture of PDMS elastomer and curing agents was thoroughly mixed and degassed in a desiccator with a mechanical vacuum pump for about 20 min to remove any air bubbles in the mixture. Next, the PDMS prepolymer was poured into PDMS chamber of PMMA base from its cast hole (Fig. 1d). After treating PDMS prepolymer at a temperature of 35 °C overnight (Fig. 1e), the PMMA–PDMS hybrid flow cell were then released from the PMMA mold and metal holder (Fig. 1f). As PDMS does not adhere to the native PMMA, the flow cell can be easily demolded without using any releasing agents. The inlet and outlet of PDMS microfluidic layer were then mechanically drilled at the edges of PDMS wraparound microchannel.

### 2.4. Strength test experiment

#### 2.4.1. Adhesion strength test of plastic–PDMS interface

To demonstrate that our PECVD $SiO_2$ intermediate layer is a universal technology for the PDMS adhesion to plastic substrates, we examine the adhesion strength of PDMS to $SiO_2$-coated PMMA, PC and COC plates, which are typically applied for a variety of microfluidic chips (Suzuki et al., 2007; Liu et al., 2009; Luna-Vera and Alvarez, 2010). The adhesion strength between the PDMS and $SiO_2$-coated plastic substrates was measured according to the previous report (Eddings et al., 2008). One 2.5 mm thick PDMS layer was first cast and solidified on one 20 mm long × 20 mm wide, 2 mm thick plastic sheet coated with 200 nm $SiO_2$ layer. Then, one 1.0 mm diameter tubing inlet hole was carefully drilled on the plastic sheet, but not through PDMS layer, to expose the plastic–PDMS interface. One metal tube was mounted into the hole and glued by an epoxy for the connection of air pressure. The pressure was slowly increased until the PDMS layer detached from the plastic substrate, at which point the pressure was recorded ($N = 4$). A negative control experiment was also performed by repeating the same experiment procedures on the native plastic substrates, whose surfaces were not deposited with any $SiO_2$ thin film by PECVD.

#### 2.4.2. Liquid leakage test of the reversible sealing interface

The maximum pressure that the reversible sealing hard–soft biosensor flow cell/SPR array chip stack could withstand was determined under flow conditions according to the previous report (Bart et al., 2009). The flow of DI-water containing some drops of red ink (used for visualization purposes) through the microchannel was slowly increased until leakage was observed, at which point the pressure was recorded ($N = 4$).

### 2.5. SPR imaging biosensor and its array chip

#### 2.5.1. SPR imaging instrument

Our SPR imaging experiment was performed on our home-made SPR imaging biosensor, which was working with Kretschmann configuration to achieve the resonant condition by total internal reflection in Fig. S1, Supporting Information (Cui et al., 2006, 2007). The hard–soft microfluidic-based biosensor flow cell, which reversibly bonded with SPR array chip, was mounted on the triangular prism of SPR imaging biosensor for SPR imaging. An intensity-stabilized, He–Ne laser with a wavelength of 650 nm was used as a light source. The laser beam was expanded and collimated by optical lens before traveling through a triangular prism and the SPR array chip. The reflected light was detected by a charge-coupled device (CCD) detector. Data were collected and displayed using an in-house Labview (National Instruments, Austin, TX, USA) program allowing for acquiring, imaging, recording, and processing images. The SPR imaging biosensor meets the requirements of the real-time kinetic studies involved in biomolecular interaction analysis. Intensity changes in regions of interest selected from the image were monitored as a function of time to generate real-time response curves.

#### 2.5.2. SPR array chip preparation

The Cr/Au (2 nm/50 nm) metallic multilayer of SPR array chips (3 × 5) was deposited on the microscope glass slide by using a sputtering deposition process. Prior to depositing the metallic film, the microscope slides were cleaned in boiling piranha solution ($H_2SO_4$:$H_2O_2$, 3:1) 20 min (Caution!) and dry at room temperature. The gold patterns array was then obtained by standard photolithographic techniques and classical lift-off technique.

The protein immobilization on the surface of SPR array chip was carried out according to the previous report (Lofas and Johnsson, 1990). To activate the carboxymethyldextran on the chip surface, the chip was immersed a mixture of 0.2 M EDC and 0.05 M NHS (1:1; v/v) for 6 min at room temperature. After washing with PBS and drying with nitrogen, a high precision microarray spotter (Institute of Electrical Engineering, Chinese Academy of Sciences) was used to spot the proteins on the SPR array surface. The SPR array chip was incubated in a humidity chamber at room temperature, to prevent drying of the spotted droplets during the 1 h immobilization process. After immobilization, the remaining active groups of the sensor surface were quenched with ethanolamine (1 M, pH 8.0) for 10 min at room temperature.

## 3. Results and discussion

### 3.1. Effect of different parameters on adhesion strength of plastic–PDMS

#### 3.1.1. Thickness of PECVD $SiO_2$ thin film

PECVD $SiO_2$ thin film has some excellent properties such as hardness, chemical-resistance, anti-corrosion and also optical, dielectric properties, so PECVD has been utilized widely to produce $SiO_2$ coatings on polymer substrates due to its low temperature, cheap processing, improved coverage, and suitable to obtain homogeneous films on a large area substrates (Reed et al., 2001). Its surface composition and characterization have been extensively studied by many researchers using a variety of techniques like Fourier transform infrared spectrometer (FT-IR), X-ray photoelectron spectrometer (XPS), etc., and the silanol groups (Si–OH) have been observed on its surface (Inoue and Takai, 1996; Teshima et al., 2002). Here, we used the PECVD $SiO_2$ thin film as an intermediate layer for irreversibly adhering PDMS to plastic substrate. IR absorption in the PECVD $SiO_2$ film at approximately 950 and 1080 $cm^{-1}$ were associated with Si–OH and Si–O–Si groups, respectively (Fig. S3, Supporting Information). We attributed the high strength bonding to silanol group condensation and strong covalent siloxane (Si–O–Si) bonds formation between PDMS and $SiO_2$ on plastic substrate (Bhattacharya et al., 2007). We also observed

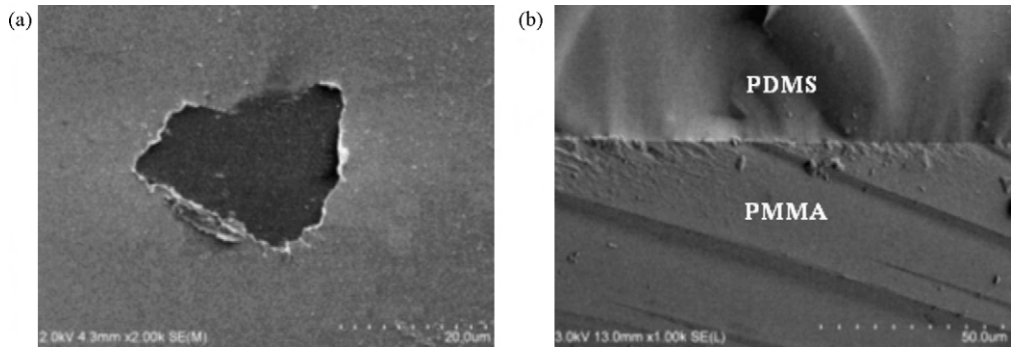


**Fig. 2.** (a) SEM image of PECVD $SiO_2$ thin film on PMMA substrate; (b) SEM image of the cross-section of PDMS and $SiO_2$-coated PMMA substrate, where an irreversible, high strength adhesion was formed under the help of $SiO_2$ intermediate layer.

that the PECVD $SiO_2$ film showed an increase in water contact angle, and a decrease in the adhesion strength to PDMS with time, which may be attributed to the rearrangement of surface chains and the presence of dangling bonds (Bhattacharya et al., 2007). Fig. 2a was SEM image of a 200 nm $SiO_2$ thin film, which was deposited on the PMMA substrate by PECVD. Fig. 2b showed the SEM image of the cross-section of PDMS and $SiO_2$-coated PMMA substrate, where the irreversible, high strength adhesion of PMMA and PDMS was formed under the help of $SiO_2$ intermediate layer. The effect of the thickness of $SiO_2$ intermediate layer on the adhesion strength of PDMS to PMMA substrate was also studied by varying the thickness of the $SiO_2$ thin film from 0 to 400 nm. When the thickness of the $SiO_2$ film increased, the adhesion strength increased and reached a relatively stable value at 200 nm thickness (Fig. S2, Supporting Information). Further increase of the $SiO_2$ film thickness did not improve the adhesion strength significantly.

Because the PECVD $SiO_2$ dry deposition process is (i) independent of the chemical composition of the substrate, (ii) suitable to three-dimensional (3-D) microstructure, (iii) can be controlled on demand, and (iv) eliminates the use of liquid chemical solvents that need to be applied in previously reported plastic–PDMS bonding technology (Lee and Ram, 2009), it may have important technological implications for rapidly fabricating a variety of hard–soft microfluidic devices for various applications.

### 3.1.2. Plastic substrates

Fig. 3 shows the adhesion strength of PDMS to three different plastic substrates with or without $SiO_2$ coating. From the experimental results, we could find that the adhesion strength of PDMS to three $SiO_2$-coated plastic substrates varied from approximately 411 to 510 kPa, which were comparable to those of samples bonded by organofunctional silanes coating method (Lee and Ram, 2009). On the contrary, all three native plastic substrates yielded a poor adhesion quality with PDMS. Therefore, the well-adherent $SiO_2$ coating on the plastic substrates plays a critical role in high strength plastics–PDMS bonding.

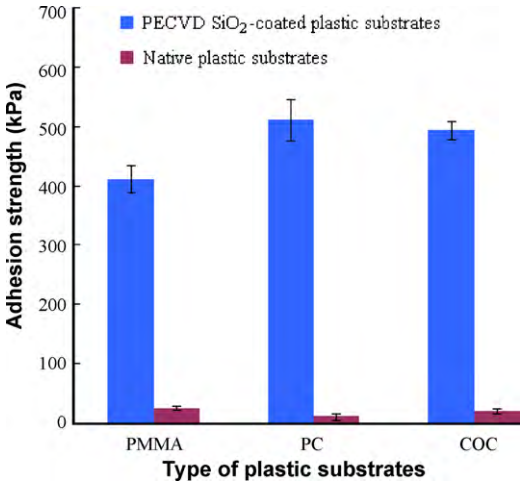


**Fig. 3.** Adhesion strength of PDMS to three plastic substrate materials including PMMA, PC and COC.

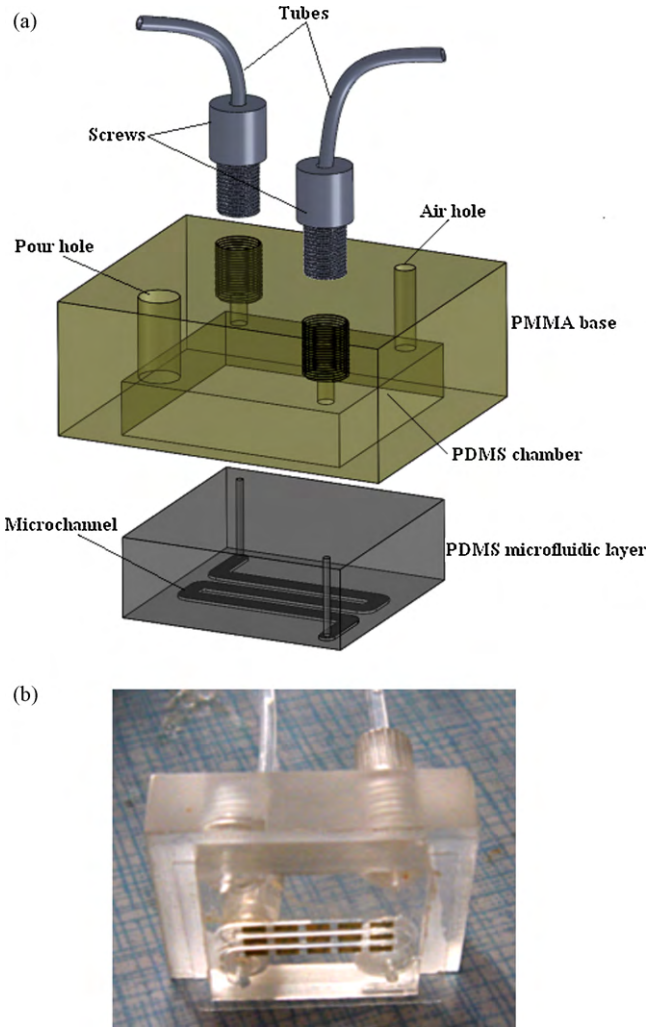


**Fig. 4.** (a) A schematic illustration of hard–soft SPR biosensor flow cell, which consists of one rigid, CNC-machined PMMA base, one flexible PDMS microfluidic layer, plastic screws and PTFE pipes; (b) photograph of hard–soft SPR biosensor flow cell/SPR array chip stack, where SPR array chip was reversibly adhered to form a sealed microfluidic network.

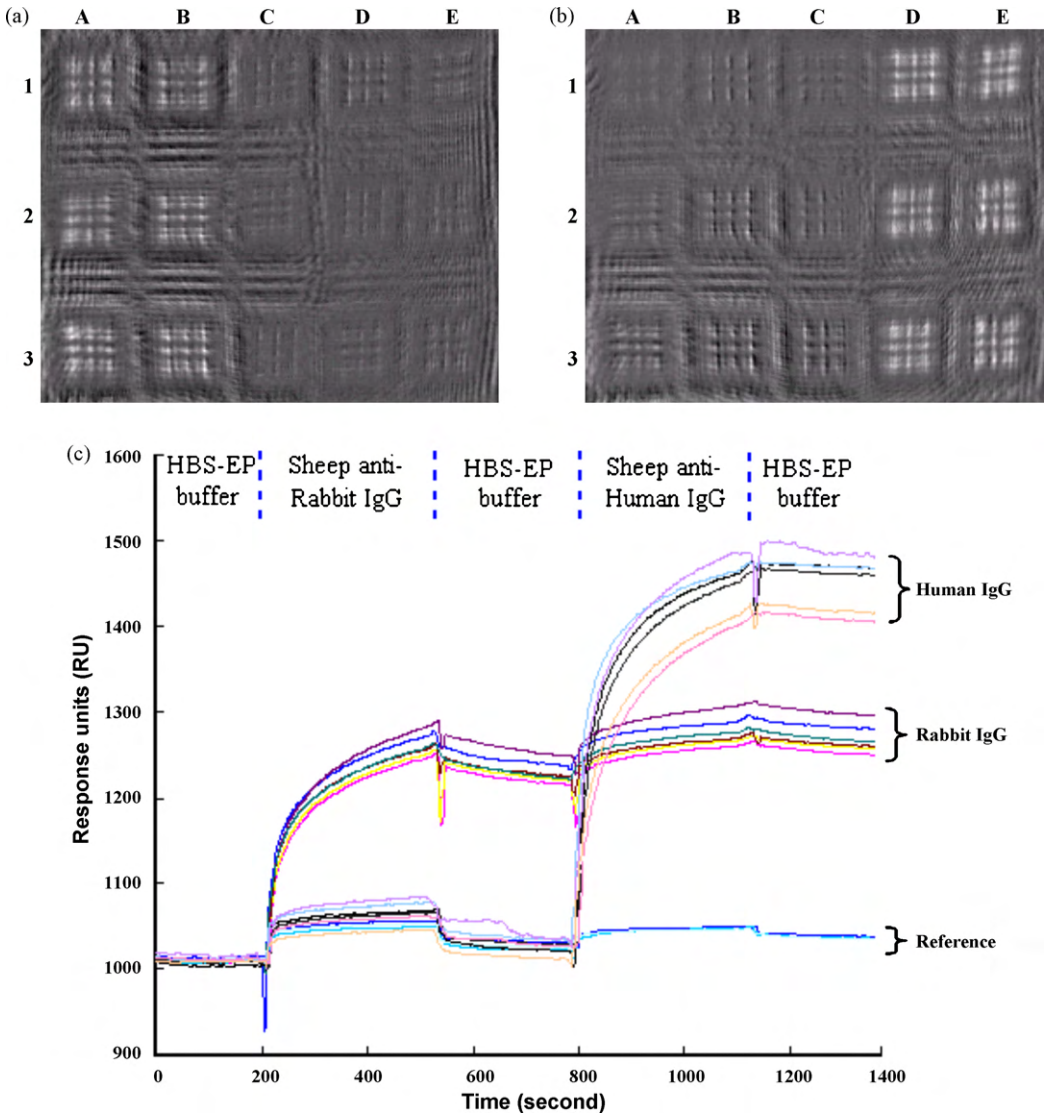


**Fig. 5.** (a) Surface plasmon resonance difference images of a SPR array chip after the introduction of sheep anti-rabbit IgG injection. Lines A and B were immobilized with rabbit IgG; line C a reference; and lines D and E were immobilized with human IgG, respectively. (b) Surface plasmon resonance difference images of a SPR array chip after the introduction of sheep anti-human IgG injection. (c) Sensorgrams recorded simultaneously during immunoreactions of anti-rabbit IgG to rabbit IgG and anti-human IgG to human IgG, in a microarray format.

### 3.1.3. *Thermal treatment temperature*

As the thermal expansion coefficient of plastic substrate materials, PDMS and PECVD $SiO_2$ intermediate layer is totally different, the thermal treatment temperature of PDMS prepolymer has a significant influence on the adhesion quality of PDMS to plastic. For example, when the temperature was above 65 °C, the PDMS layer tended to detach from the PMMA substrate after cooling to the room temperature. Therefore, a relatively low temperature was required in the course of PDMS solidification. In our experiment, PDMS prepolymer was treated either at 35 °C overnight or at room temperature for 24 h.

## 3.2. *Hard–soft microfluidic-based biosensor flow cell*

Fig. 4a is a schematic illustration of our hard–soft SPR biosensor flow cell, which consists of one rigid, CNC-machined PMMA base, one flexible PDMS microfluidic layer, plastic screws and PTFE pipes. The top of the rigid PMMA base has a thread inlet and outlet for rapid tubing connection, cast hole for PDMS pouring, and air hole for venting purposes. The PDMS layer has a wraproundmicrofluidic channel, and can reversibly adhere to SPR array chip for forming a sealed microfluidic network. The wraproundfluidic design of SPR biosensor flow cell also ensures nearly uniform fluid to flow through SPR array surface and avoids the air bubbles. Fig. 4b shows a photograph of a reversibly sealing hard–soft SPR biosensor flow cell/SPR array chip stack. This novel hard–soft biosensor microfluidic flow cell does not only keep the original advantage of conventional PDMS-based flow cell such as the intrinsically soft interface, easy-to-fabrication, and low cost, but also has a rigid, robust, easy-to-use interface to tubing connection, which will, for example, enable the biosensors to be used outside of the laboratory by relatively untrained users for food analysis, point-of-care medical applications, etc.

## 3.3. *Liquid leakage test of the reversibly sealed hard–soft biosensor flow cell*

In our SPR imaging experiment, we reversibly bonded SPR array chip to our hard–soft microfluidic-based biosensor flow cell by bringing them into contact to form a closed channel, and then

mounted this stack on our home-made SPR imaging biosensor. Therefore, the maximum pressure our reversibly sealed hard–soft SPR biosensor flow cell/array chip stack could withstand was our first consideration. Here, we evaluated the maximum pressure endurance of this stack by liquid leakage test experiment. Our experimental result showed that this hard–soft biosensor flow cell/array chip stack could be operated up to 185 ± 19 kPa ($N$ = 4) in aqueous environments without failure, which was more than 5 times higher than that of the reversible sealing glass-PDMS microfluidic chip reported in the previous literature (McDonald et al., 2000). It should be attributed to the "hard–soft–hard" sandwich stack structure, where the soft PDMS microfluidic layer was tightly sandwiched between rigid PMMA base and rigid SPR array chip, and the distortion of PDMS microchannel could not occur easily even under high pressure. The high pressure endurance of 185 kPa was clearly high enough for use in many microfluidic-based biosensor flow cell, including high-flow rate applications, as pressures in most microfluidic systems only occasionally exceed 100 kPa.

### 3.4. Applications in SPR imaging detection

#### 3.4.1. Real-time monitoring of the immunoglobulin G (IgG) interaction

A model involving the interaction of anti-rabbit IgG to rabbit IgG, and anti-human IgG to human IgG was used to verify the real-time monitoring capability of the developed hard–soft microfluidic-based biosensor flow cell. SPR array chip immobilized with rabbit IgG and human IgG were reversibly bonded to the flow cell, and then coupled with our home-made SPR imaging biosensor. Next, the flow cell was connected to automatic manipulator/multivalves by its macro-to-micro interface using PTFE pipes and screws for the liquid solution transportation. The HBS-EP buffer and sample solution were introduced into the hard–soft microfluidic-based biosensor flow cell with a constant rate of 25 μL/min. The whole detection procedure was described as follows: 0–200 s for HBS-EP buffer injection, 201–500 s for 1.2 mg/mL sheep anti-rabbit IgG injection, 501–800 s HBS-EP buffer washing, 801–1100 for 0.5 mg/mL sheep anti-human IgG injection, and 1101–1400 s for buffer washing, respectively.

Shown in Fig. 5a and b is, respectively, SPR difference images of sheep anti-rabbit IgG and sheep anti-human IgG, obtained by subtracting the images taken before and after exposing the SPR array chip to the protein solution (Wegner et al., 2003). From these SPR difference images, the IgGs specific interactions are clearly observed on the SPR array chip with little nonspecific adsorption. Fig. 5c was the sensorgrams recorded simultaneously during immunoassay of anti-rabbit IgG to rabbit IgG and anti-human IgG to human IgG, in an array format. The experimental results demonstrate that our hard–soft microfluidic-based biosensor flow cell can successfully be applied to detect the phase variation caused by antibodies adsorbed on the Au array surface, and shows a high-throughput screening capabilities.

#### 3.4.2. Detection of sulfamethoxazole and sulfamethazine

Sulfonamides, a family of broadspectrum synthetic bacteriostatic antibiotics, are commonly given to feed animals for prophylactic or therapeutic purposes. Abuse of these drugs in animal breeding will lead to unwanted residues in food of animal origin. Therefore, it has very important significance to develop a rapid, sensitive, and high-throughput technology to detect them (Wang et al., 2006). SPR biosensors have proven themselves versatile, robust and capable of producing rapid and reliable results for the analysis of drug residues in complex matrices with minimal sample preparation (Shankaran et al., 2007). Here, we detect the sulfamethoxazole and sulfamethazine on our hard–soft microfluidic-based biosensor flow cell coupled with the SPR imaging biosensor.

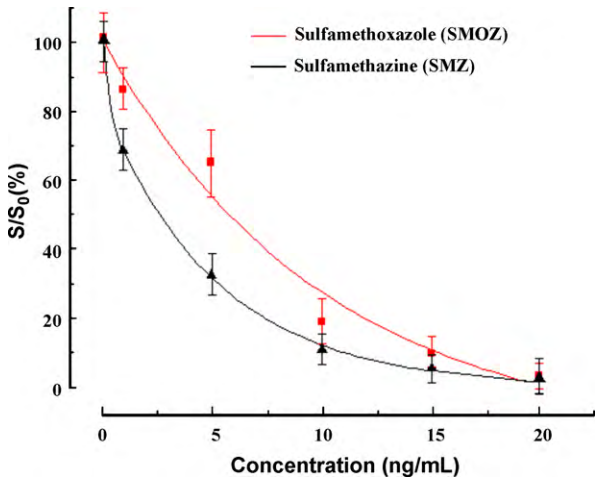


**Fig. 6.** Calibration curves for the detection of sulfamethoxazole and sulfamethazine on hard–soft microfluidic-based biosensor flow cell coupled with SPR imaging biosensor. The binding slope at each sulfamethoxazole and sulfamethazine concentration ($S$) was divided by the antibody binding slope determined in the presence of zero sulfamethoxazole and sulfamethazine concentration ($S_0$) to give a normalized binding response ($S/S_0$).

In this study, an inhibition immunoassay method was used to detect sulfamethoxazole and sulfamethazine (Bienenmann-Ploum et al., 2005; Dillon et al., 2005). Firstly, sulfamethoxazole standard was prepared in PBS buffer at the concentration of 0, 2, 10, 20, 30 and 40 ng/mL. Each sample was incubated separately with an equal volume of a 50-fold dilution of the sulfamethoxazole antibody for 5 min at 37 °C. Then, sample solution was passed consecutively over SPR array chip immobilized with sulfamethoxazole–BSA at a flow rate of 25 μL/min. This was followed by the surface regeneration with 0.1 M $H_3PO_4$. The slope of the 50-s injection pulse was used as a measure of response. To normalize the results from individual assays, the binding slope at each sulfamethoxazole concentration ($S$) was divided by the antibody binding slope determined in the absence of sulfamethoxazole ($S_0$) to yield a normalized binding response ($S/S_0$) (Dillon et al., 2005). Sulfamethazine was also detected using the same procedure.

The calibration curves in Fig. 6 for sulfamethoxazole and sulfamethazine detection were constructed by plotting their mean $S/S_0$ against their concentration. The RSD of $S/S_0$ in the absence of sulfamethoxazole and sulfamethazine was 9% and 6%, respectively, and the limits of detection of sulfamethoxazole and sulfamethazine were calculated as 3.5 and 0.6 ng/mL, respectively, which were comparable to commercial Biacore SPR biosensor (Bienenmann-Ploum et al., 2005).

## 4. Conclusions and outlook

In this study, we successfully developed a hard–soft, novel, compact microfluidic-based biosensor flow cell for SPR imaging immunoassay, by using PECVD $SiO_2$ film as an adhesion intermediate layer. This novel hard–soft flow cell does not only keep the original advantage of conventional PDMS-based flow cell such as the intrinsically soft interface, easy-to-fabrication, and low cost, but also has a rigid, robust, easy-to-use interface to tubing connection.

The irreversible adhesion of various plastic substrates with PDMS was demonstrated by employing PECVD $SiO_2$ film as an adhesion intermediate layer. Owing to its simple, low cost and suitability for high-throughput production, this method was widely applicable to a variety of plastic–PDMS microfluidic devices for various applications. Moreover, "hard–soft–hard" sandwich stack structure

of our hard–soft biosensor flow cell/SPR array chip enables their reversible sealing interface to withstand a high pressure of up to 185 kPa.

The performance of our hard–soft microfluidic-based biosensor flow cell was successfully demonstrated with two types of SPR experiments: the real time monitoring of IgGs interaction, as well as the detection of sulfamethoxazole and sulfamethazine with the sensitivity of 3.5 and 0.6 ng/mL, respectively, which have shown a high sensitivity and a high-throughput screening capabilities. Its application for SPR imaging biosensor flow cell was merely an example. We anticipate that this novel hard–soft microfluidic device and its fabrication method are also useful for a variety of other biosensor flow cells (Yoshinobu et al., 2005; Michalzik et al., 2005; Mitsakakis et al., 2009).

## Acknowledgments

This present work was supported, in part, by the National Natural Science Foundation of China (Grant Nos. 60427001 and 60501020), National High Technology Research and Development Program of China (Grant No. 2006AA04Z355) and Scientific Research Startup Special Foundation on Excellent Ph.D. Thesis and Presidential Award of the Chinese Academy of Sciences.

## Appendix A. Supplementary data

Supplementary data associated with this article can be found, in the online version, at doi:10.1016/j.bios.2010.06.041.

## References

Bart, J., Tiggelaar, R., Yang, M., Schlautmann, S., Zuilhof, H., Gardeniers, H., 2009. Lab Chip 9, 3481–3488.
Bhattacharya, S., Gao, Y., Korampally, V., Othman, M.T., Grant, S.A., Gangopadhyay, K., Gangopadhyay, S., 2007. Appl. Surf. Sci. 253, 4220–4225.
Bienenmann-Ploum, M., Korpimaki, T., Haasnoot, W., Kohen, F., 2005. Anal. Chim. Acta 529, 115–122.
Chow, W.W.Y., Lei, K.F., Shi, G., Li, W.J., Huang, Q., 2006. Smart Mater. Struct. 15, S112–S116.
Crevillén, A.G., Avila, M., Pumera, M., Gonzalez, M.C., Escarpa, A., 2007. Anal. Chem. 79, 7408–7415.
Cui, D., Cai, H., Wang, J., Li, Y., Liang, J., Liu, C., Wang, Y., Zheng, Z., 2006. Chinese Patent Appl. No. CN 200610066542.4.
Cui, D., Liang, J., Cai, H., Wang, J., Li, Y., Wang, Y., Liu, C., Zheng, Z., 2007. Prog. Nat. Sci. 17, 93–98.
Dillon, P.P., Killard, A.J., Daly, S.J., Leonard, P., O'Kennedy, R., 2005. J. Immunol. Methods 296, 77–82.
Eddings, M.A., Johnson, M.A., Gale, B.K., 2008. J. Micromech. Microeng. 18, 067001 (4 pp).
Gervais, L., Delamarche, E., 2009. Lab Chip 9, 3330–3337.
Inoue, Y., Takai, O., 1996. Plasma Sources Sci. Technol. 5, 339–343.
Kawazumi, H., Gobi, K.V., Ogino, K., Maeda, H., Miura, N., 2005. Sens. Actuators B 108, 791–796.
Kersey, L., Ebacher, V., Bazargan, V., Wang, R., Stoeber, B., 2009. Lab Chip 9, 1002–1004.
Kjeang, E., Roesch, B., McKechnie, J., Harrington, D.A., Djilali, N., Sinton, D., 2007. Microfluid. Nanofluid. 3, 403–416.
Lee, K.S., Ram, R.J., 2009. Lab Chip 9, 1618–1624.
Lee, K.H., Su, Y.D., Chen, S.J., Tseng, F.G., Lee, G.B., 2007. Biosens. Bioelectron. 23, 466–472.
Li, H., Lin, J., 2009. Anal. Bioanal. Chem. 393, 555–567.
Liu, C., Cui, D., Chen, X., 2007. J. Chromatogr. A 1170, 101–106.
Liu, C., Qiu, X., Ongagna, S., Chen, D., Chen, Z., Abrams, W., Malamud, D., Corstjens, P., Bau, H.H., 2009. Lab Chip 9, 768–776.
Liu, R.H., Munro, S.B., Nguyen, T., Siuda, T., Suciu, D., Bizak, M., Slota, M., Fuji, H.S., Danley, D., McShea, A., 2006. J. Assoc. Lab. Autom. 11, 360–367.
Lofas, S., Johnsson, B., 1990. J. Chem. Soc. Chem. Commun. 211, 1526–1528.
Luna-Vera, F., Alvarez, J.C., 2010. Biosens. Bioelectron. 25, 1539–1543.
Luo, Y., Yu, F., Zare, R.N., 2008. Lab Chip 8, 694–700.
McDonald, J.C., Duffy, D.C., Anderson, J.R., Chiu, D.T., Wu, H., Schueller, O.J.A., Whitesides, G.M., 2000. Electrophoresis 21, 27–40.
Michalzik, M., Wilke, R., Büttgenbach, S., 2005. Sens. Actuators B 111–112, 410–415.
Mitsakakis, K., Tserepi, A., Gizeli, E., 2009. Microelectron. Eng. 86, 1416–1418.
Nakajima, H., Harada, Y., Asano, Y., Nakagama, T., Uchiyama, K., Imato, T., Soh, N., Hemmi, A., 2006. Talanta 70, 419–425.
Pihl, J., Karlsson, M., Chiu, D.T., 2006. Drug Discov. Today 10, 1377–1383.
Reed, H.A., White, C.E., Rao, V., Allen, S.A.B., Henderson, C.L., Kohl, P.A., 2001. J. Micromech. Microeng. 11, 733–737.
Samel, B., Chowdhury, M.K., Stemme, G., 2007. J. Micromech. Microeng. 17, 1710–1714.
Shankaran, D.R., Gobi, K.V., Miura, N., 2007. Sens. Actuators B 121, 158–177.
Suzuki, H., Tabata, K.V., Noji, H., Takeuchi, S., 2007. Biosens. Bioelectron. 22, 1111–1115.
Tang, L., Lee, N.Y., 2010. Lab Chip 10, 1274–1280.
Teshima, K., Inoue, Y., Sugimura, H., Takai, O., 2002. Vacuum 66, 353–357.
Tsao, C.W., DeVoe, D.L., 2009. Microfluid. Nanofluid. 6, 1–16.
Varshney, M., Li, Y., Srinivasan, B., Tung, S., 2007. Sens. Actuator B 128, 99–107.
Vlachopoulou, M.E., Tserepi, A., Pavli1, P., Argitis, P., Sanopoulou, M., Misiakos, K., 2009. J. Micromech. Microeng. 19, 015007 (6 pp).
Wang, S., Zhang, H.Y., Wang, L., Duan, Z.J., Kennedy, I., 2006. Food Addit. Contam. 23, 362–384.
Wegner, G.J., Lee, H.J., Marriott, G., Corn, R.M., 2003. Anal. Chem. 75, 4740–4746.
Wheeler, R., Chah, S., Whelan, R.J., Zare, R.N., 2004. Sens. Actuators B 98, 208–214.
Wu, H., Huang, B., Zare, R.N., 2005. Lab Chip 5, 1393–1398.
Wuu, D.S., Lo, W.C., Chang, L.S., Horng, R.H., 2004. Thin Solid Films 468, 105–108.
Yager, P., Edwards, T., Fu, E., Helton, K., Nelson, K., Tam, M.R., Weigl, B.H., 2006. Nature 442, 412–418.
Yoshinobu, T., Iwasaki, H., Ui, Y., Furuichi, K., Ermolenko, Y., Mourzina, Y., Wagner, T., Näther, N., Schöning, M.J., 2005. Methods 37, 94–102.